Procyanidin B2 suppresses hyperglycemia-induced renal mesangial cell dysfunction by modulating CAV-1-dependent signaling

JUN YIN[1,2], KE WANG[3], XUE ZHU[3], GUOYUAN LU[1], DONGHUA JIN[4], JUNSI QIU[2] and FANFAN ZHOU[5]

[1]Department of Nephrology, The First Affiliated Hospital of Soochow University, Suzhou, Jiangsu 215006; [2]Department of Nephrology, The Affiliated Wuxi No.2 People's Hospital of Nanjing Medical University, Wuxi, Jiangsu 214002; [3]NHC Key Laboratory of Nuclear Medicine, Jiangsu Key Laboratory of Molecular Nuclear Medicine, Jiangsu Institute of Nuclear Medicine, Wuxi, Jiangsu 214063; [4]Department of Nephrology, People's Hospital of Suzhou New District, Suzhou, Jiangsu 215129, P.R. China; [5]Sydney Pharmacy School, The University of Sydney, Sydney, New South Wales A-2006, Australia

Received March 10, 2022; Accepted May 27, 2022

DOI: 10.3892/etm.2022.11423

Abstract. The dysfunction of renal mesangial cells (MCs) is a hallmark of diabetic kidney disease (DKD), which triggers glomerulosclerosis leading to end-stage renal disease. Procyanidin B2 (PB2), the main component of proanthocyanidin, is well known for its antioxidant and anti-inflammatory effects; however, it remains unclear as to whether it has protective effects on DKD. The present study investigated the protective effect of PB2 against hyperglycemia-induced renal MC dysfunction in mouse SV40-Mes13 (Mes13) cells. The Mes13 cells were treated with or without PB2 under HG conditions. Cell proliferation was assessed using an MTT assay and oxidative stress was assessed by examining intracellular ROS generation and H_2O_2 production. The changes in extracellular matrix accumulation- and cellular inflammation-related proteins were measured by western blot analysis, ELISA and immunofluorescence analysis. The results showed that PB2 treatment markedly attenuated hyperglycemia-induced cell proliferation, oxidative stress, extracellular matrix accumulation and cellular inflammation in Mes13 cells, which was accompanied by an inactivation of redoxosomes, TGF-β1/SMAD and IL-1β/TNF-α/NF-κB signaling pathways. The present study also demonstrated that hyperglycemia upregulated and activated caveolin-1 (CAV-1), whereas PB2 treatment potently reversed this effect. In accordance, CAV-1 overexpression abolished the protective effects of PB2 against hyperglycemia in Mes13 cells, indicating that the cytoprotective effect of PB2 was CAV-1-dependent. These findings form the basis of the potential clinical applications of PB2 in the treatment of DKD.

Correspondence to: Dr Guoyuan Lu, Department of Nephrology, The First Affiliated Hospital of Soochow University, 899 Pinghai Road, Suzhou, Jiangsu 215006, P.R. China
E-mail: luguoyuan@medmail.com.cn

Dr Donghua Jin, Department of Nephrology, People's Hospital of Suzhou New District, 95 Huashan Road, Suzhou, Jiangsu 215129, P.R. China
E-mail: dhjin18@sina.com

Key words: diabetic kidney disease, renal mesangial cells, procyanidin B2, caveolin-1

Introduction

Diabetic kidney disease (DKD) (also known as diabetic nephropathy) has been reported to develop in ~40% of patients with diabetes worldwide and is the primary cause of end-stage renal disease (1,2). The morphological characteristics of DKD include excessive deposition of extracellular matrix (ECM) with mesangial expansion, thickening of glomerular and tubular basement membranes, podocyte effacement and tubulointerstitial fibrosis (3). Mesangial cells (MCs) are the main cellular constituents of the glomerular mesangium, accounting for ~35% of the total cells in the glomerulus (4). The main function of glomerular MCs includes supporting structural architecture of the glomerular capillary, maintaining mesangial matrix homeostasis and regulating the filtration surface area (5,6). Under hyperglycemia, these cells may undergo overproliferation with increasing synthesis of ECM proteins, which leads to glomerulosclerosis in the occurrence and development of DKD (7). Therefore, an improved understanding of the role of MCs in the pathogenesis of DKD may contribute to the development of novel therapeutic drugs for the control of this disease.

Caveolae are small glycosphingolipid- and cholesterol-enriched omega-shaped invaginations of the plasma membrane (50-100 nm), which have a wide range of functions, such as endocytosis, transcytosis, and regulation of cell differentiation, proliferation and apoptosis (8,9). Caveolin-1 (CAV-1) is an integral membrane protein required for caveolae formation, and previous studies have suggested its important role in the pathogenesis of DKD (10,11). It has been confirmed that CAV-1 can promote the synthesis and accumulation of the ECM in MCs under hyperglycemia by activating several

profibrotic pathways (12). In addition, CAV-1 has been shown to be involved in the upregulation of NADPH oxidase (NOX) activity and production of superoxide in response to high glucose (HG) in MCs (13). Thus, increasing evidence has indicated a pathogenic role of CAV-1/caveolae in DKD, which may become a novel and potent therapeutic target for this disease.

Proanthocyanidin is widely distributed in plants and is the active ingredient in grape seed, green and black tea, wolfberry and fruit juices (14). It has been reported that proanthocyanidin has biological activities, including free radical-scavenging, antioxidant, anti-inflammatory and antitumor properties (14,15). Procyanidin B2 (PB2), the main component of proanthocyanidin, is composed of two molecules of flavan-3-ol (-)-epicatechin linked by a C4-C8 bond. PB2 has been reported to prevent reactive oxygen species (ROS) generation and inhibit inflammation (16). In addition, previous studies have indicated the protective effect of PB2 on DKD (17,18). However, little is currently known about the molecular mechanism underlying the protective effect of PB2 on DKD. The present study aimed to investigate the cytoprotective effects of PB2 against cell proliferation, oxidative stress, ECM accumulation and inflammation in renal MCs, and explored the molecular mechanism associated with such effects.

Materials and methods

Chemicals and reagents. PB2 (purity>99%), NSC23766, VAS2870 and LY2109761 were purchased from MedChemExpress. Chemicals, such as MTT and DMSO, were obtained from MilliporeSigma. The following antibodies were obtained from Abcam: Phosphorylated (p)-VAV2 (cat. no. ab86695), VAV2 (cat. no. ab52640), RAC1 (cat. no. ab155938), NOX4 (cat. no. ab133303), collagen IV (cat. no. ab6586), fibronectin (cat. no. ab268020), TGF-β1 (cat. no. ab215715), p-SMAD2/3 (cat. no. ab272332), SMAD2/3 (cat. no. ab217553), CAV-1 (cat. no. ab32577), p-CAV-1 (cat. no. ab75876), NF-kB p65 (cat. no. ab16502), goat anti-rabbit IgG H&L (HRP) (cat. no. ab7090) and goat anti-mouse IgG H&L (HRP) (cat. no. ab205719), goat anti-rabbit IgG H&L (Alexa Fluor 647) (cat. no. ab150079) and GAPDH (cat. no. sc-365062) was obtained from Santa Cruz Biotechnology, Inc. The RAC1 activity assay kit (cat. no. STA-401-1) was obtained from Cell Biolabs, Inc. Other chemicals and reagents used in the present study, unless otherwise specified, were obtained from Beyotime Institute of Biotechnology or Sangon Biotech Co., Ltd.

Cell culture and treatments. The mouse mesangial SV40-Mes13 (Mes13) cells were purchased from the American Type Culture Collection. Cells were cultured in Dulbecco's modified Eagle medium (Gibco; Thermo Fisher Scientific, Inc.) supplemented with 10% (v/v) heat-inactivated fetal bovine serum (Gibco; Thermo Fisher Scientific, Inc.) at 37˚C in a humidified atmosphere (95% air, 5% CO_2). The concentration of D-glucose to induce hyperglycemia (at 37˚C for 12 h) was chosen according to previous studies (19,20), the concentration of PB2 (at 37˚C for 12 h) was chosen according to another previous study (17), and the untreated cells were chosen as a control. For evaluating the involvement of redoxosomes in the effect of PB2, cells were treated with RAC1 inhibitor (80 μM) or NOX inhibitor (10 μM) under HG conditions (25 mM) for 12 h at 37˚C, and ROS or H_2O_2 generation was assessed by ROS or H_2O_2 assay kits. For evaluating the involvement of TGF-β1/SMAD, cells were treated with TGF-β1/SMAD inhibitor (LY2109761, 10 μM) under HG conditions (25 mM) for 12 h at 37˚C. The expression levels of collagen IV and fibronectin were assessed by western blot analysis.

Cell transfection. The negative control pcDNA3.1-vector was purchased from Invitrogen; Thermo Fisher Scientific, Inc. and the CAV-1 expression vector pcDNA3.1-CAV-1 was purchased from Shanghai GenePharma Co., Ltd. Cells were seeded in 96-well plates ($1x10^4$ cells/well) or 6-well plates ($1x10^5$ cells/well), and transfected with empty or expression vector (1 μg/ml) using Lipofectamine® 2000 reagent (Invitrogen; Thermo Fisher Scientific, Inc.) at 37˚C according to the manufacturer's instructions. After 48 h, western blot analysis was performed to determine the efficiency of transfection. In addition, cells underwent subsequent experiments 48 h post-transfection.

Cell proliferation analysis. Cell proliferation was determined using the MTT assay. Cells ($1x10^4$/well) were incubated with 0.5 mg/ml MTT solution (100 μl) for 3 h at 37˚C. The cultured medium was then replaced with DMSO solution (100 μl) and the absorbance was recorded at a wavelength of 490 nm (DTX800; Beckman Coulter, Inc.).

Oxidative marker analysis. Intracellular ROS generation was assessed using a ROS assay kit (Beijing Solarbio Science & Technology Co., Ltd.) with fluorescent probe 2',7'-dichlorofluorescein diacetate (DCFH-DA). Briefly, cells ($1x10^4$/well) with or without treatment were incubated with DCFH-DA (10 μM) for 15 min at 37˚C. ROS concentration was analyzed by measuring fluorescence using a fluorescence microplate reader (SpectraMax M5; Molecular Devices, LLC) with excitation and emission wavelengths at 488 and 525 nm, respectively. Intracellular H_2O_2 levels were measured using a hydrogen peroxide/peroxidase assay kit (cat. no. BC3595; Beijing Solarbio Science & Technology Co., Ltd.) according to the manufacturer's protocol, with excitation at 530 nm and detection at 590 nm, using a fluorescence microplate reader (SpectraMax M5; Molecular Devices, LLC).

Rac1 activation assay. RAC1 activity was assessed using RAC1 activation assay kit (cat. no. STA-401-1; Cell Biolabs, Inc.) according to the manufacturer's protocol. Briefly, cells after treatment were lysed by RIPA lysis buffer and PAK PBD agarose beads were used to isolate and pull-down the active form of RAC1 (RAC1-GTP). Subsequently, the precipitated RAC1-GTP was detected by western bot analysis using RAC1 antibody.

Western blot analysis. Total protein was extracted from Mes13 cells by RIPA lysis buffer (Beyotime Institute of Biotechnology) and quantitively determined using BCA Protein Assay kit (Beyotime Institute of Biotechnology). Proteins (50 μg/lane) were loaded and separated by SDS-PAGE on 10% gels and were then transferred onto polyvinylidene difluoride membranes. Membranes were blocked with non-fat

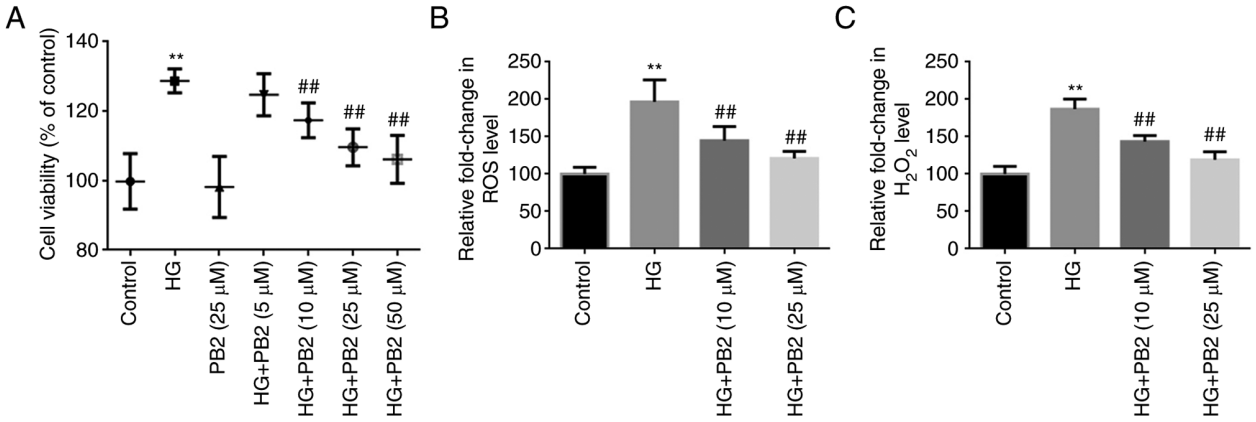

Figure 1. Protective effect of PB2 against HG-induced cell proliferation and oxidative stress in Mes13 cells. Cells were treated with PB2 (5, 10, 25 and 50 μM) under HG conditions (25 mM) for 12 h. (A) Cell proliferation was assessed by MTT assay. (B) ROS generation was assessed using a ROS assay kit and statistically analyzed. (C) H_2O_2 generation was assessed using the H_2O_2 detection kit and statistically analyzed. All data are presented as the mean ± SD of three independent experiments. **P<0.01 vs. control; $^{\#\#}$P<0.01 vs. HG. PB2, procyanidin B2; HG, high glucose; ROS, reactive oxygen species.

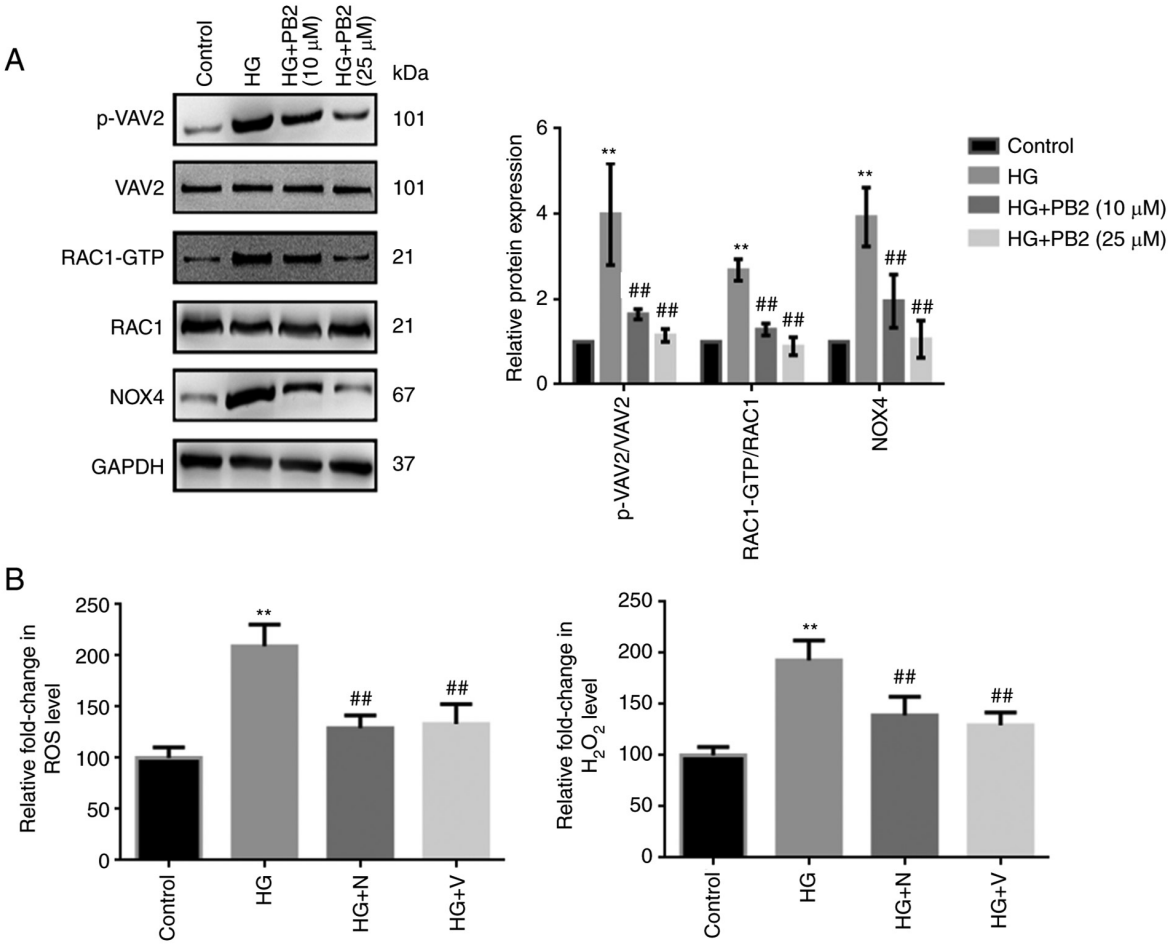

Figure 2. Regulatory effect of PB2 on redoxosomes signaling in Mes13 cells. (A) Cells were treated with PB2 (10 and 25 μM) under HG conditions (25 mM) for 12 h. The expression levels of redoxosome-related proteins were assessed by western blot analysis. (B) Cells were treated with RAC1 inhibitor (N, 80 μM) or NOX inhibitor (V, 10 μM) under HG conditions (25 mM) for 12 h at 37˚C. ROS generation was assessed using a ROS assay kit and H_2O_2 generation was assessed using the H_2O_2 detection kit, and results were statistically analyzed. All data are presented as the mean ± SD of three independent experiments. **P<0.01 vs. control; $^{\#\#}$P<0.01 vs. HG. PB2, procyanidin B2; HG, high glucose; N, NSC23766; V, VAS2870; ROS, reactive oxygen species; NOX, NADPH oxidase.

milk (5% in 0.1% Tween20-PBS buffer) for 1 h at room temperature and incubated with primary antibodies (1:1,000) overnight at 4˚C. Subsequently, membranes were incubated with HRP-conjugated secondary antibodies (1:500) for 1 h at room temperature. The bands were detected using Immobilon Western Chemiluminescent HRP Substrate (Beyotime Institute of Biotechnology) and band intensities were semi-quantified using ImageJ 1.48 (National Institutes of Health).

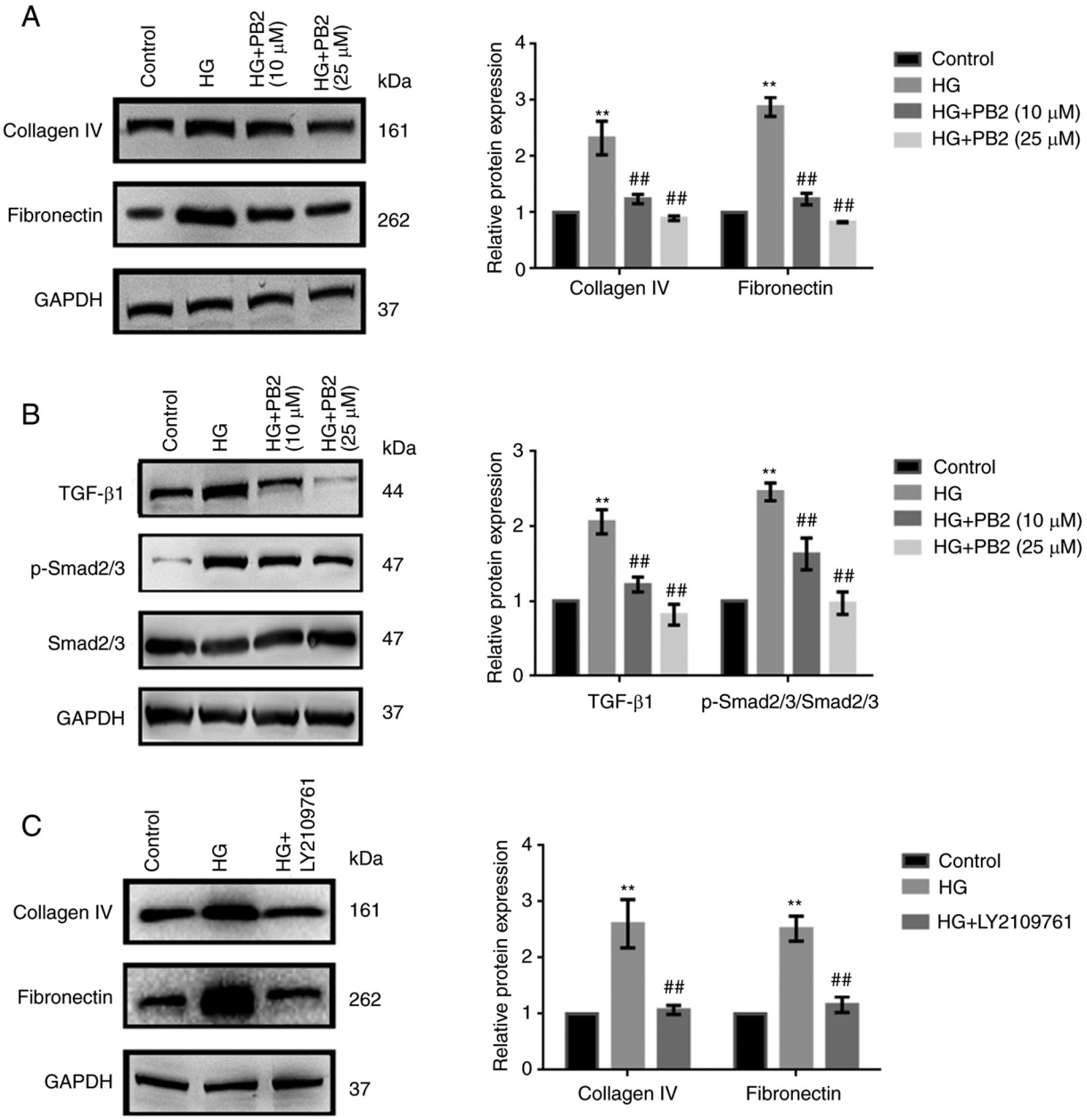

Figure 3. Protective effect of PB2 against HG-induced extracellular matrix accumulation in Mes13 cells. (A) Cells were treated with PB2 (10 and 25 μM) under HG conditions (25 mM) for 12 h. The expression levels of collagen IV and fibronectin were assessed by western blot analysis and statistically analyzed. (B) Cells were treated with PB2 (10 and 25 μM) under HG conditions (25 mM) for 12 h. The expression levels of TGF-β1/SMAD signaling-related proteins were assessed by western blot analysis and statistically analyzed. (C) Cells were treated with TGF-β1/SMAD inhibitor (LY2109761, 10 μM) under HG conditions (25 mM) for 12 h at 37˚C. The expression levels of collagen IV and fibronectin were assessed by western blot analysis and statistically analyzed. All data are presented as the mean ± SD of three independent experiments. **P<0.01 vs. control; $^{\#\#}$P<0.01 vs. HG. PB2, procyanidin B2; HG, high glucose; p-, phosphorylated.

Enzymelinked immunosorbent assay (ELISA). The cell supernatant was collected after the indicated treatment (cells with or without CAV-1 transfection were treated with PB2 (25 μM) under HG conditions (25 mM) for 12 h) and processed for ELISA analysis. Culture supernatant (100 μl) was analyzed using the ELISA kits (IL-1β and TNF-α) (Beijing Solarbio Science & Technology Co., Ltd.) according to the manufacturers' protocols. The absorbance was measured at 450 nm using a microplate reader (Molecular Devices, LLC).

Immunofluorescence analysis. Cells were fixed in 2% paraformaldehyde for 20 min at room temperature and permeabilized in 0.1% Triton X-100 for 20 min at room temperature, followed by incubation with primary antibody (NF-κB p65; 1:500) overnight at 4˚C and fluorescent-conjugated secondary antibody [goat anti-rabbit IgG H&L (Alexa Fluor 647); 1:250] for 1 h at room temperature. Fluorescence was observed with a fluorescence microscope (Leica Microsystems GmbH). DAPI (0.5 μg/ml; 20 min at room temperature) was used to stain the nuclei.

Statistical analysis. Statistical analysis was performed using SPSS 16.0 software package (SPSS, Inc.). Data are presented as the mean ± SD of three independent experiments. Statistical comparisons were made by one-way ANOVA followed by

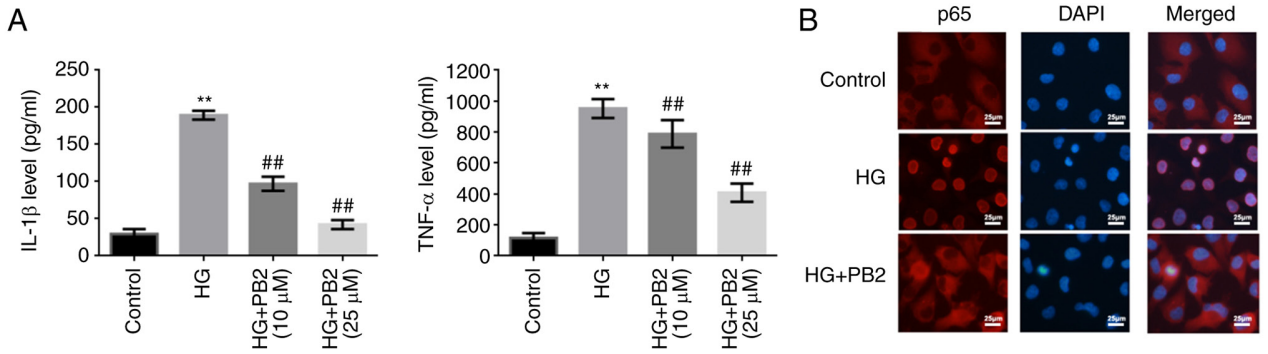

Figure 4. Protective effect of PB2 against HG-induced inflammation in Mes13 cells. Cells were treated with PB2 (10 and 25 μM) under HG conditions (25 mM) for 12 h. (A) Levels of IL-1β and TNF-α was assessed by enzyme-linked immunosorbent assay and statistically analyzed. (B) Localization of p65 (NF-κB) was assessed by immunofluorescence. Scale bar, 25 μm. All data are presented as the mean ± SD of three independent experiments. **P<0.01 vs. control; $^{\#\#}$P<0.01 vs. HG. PB2, procyanidin B2; HG, high glucose.

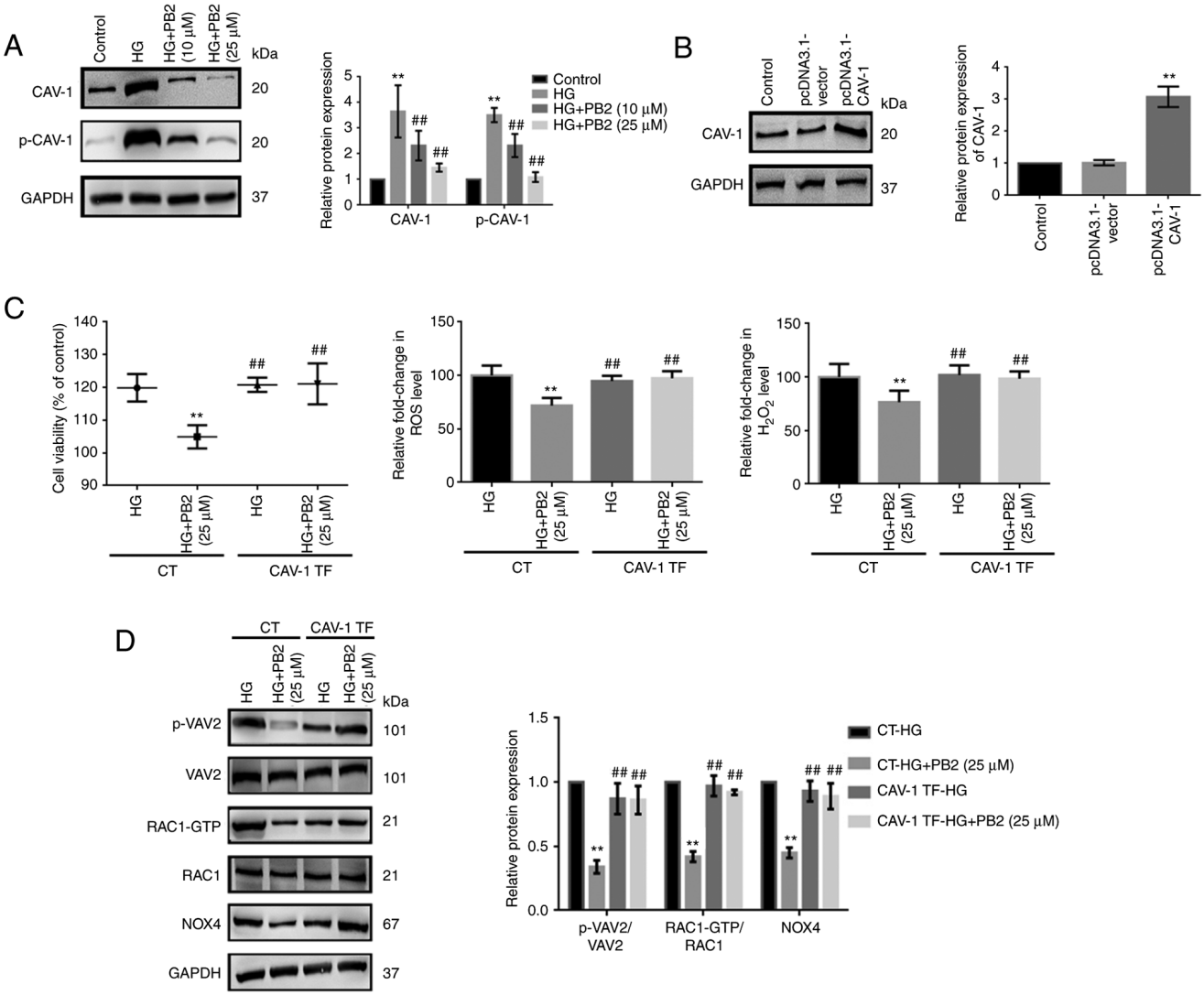

Figure 5. Effect of CAV-1 overexpression on the cytoprotective effect of PB2 against oxidative stress in Mes13 cells. (A) Cells were treated with PB2 (10 and 25 μM) under HG conditions (25 mM) for 12 h, and the expression levels of CAV-1 and p-CAV-1 were assessed by western blot analysis and statistically analyzed. **P<0.01 vs. control, $^{\#\#}$P<0.01 vs. HG. (B) Cells were transfected with pcDNA3.1-vector (negative control) or pcDNA3.1-CAV-1 for 48 h, and the expression levels of CAV-1 were assessed by western blot analysis and statistically analyzed. **P<0.01 vs. control. (C) Cells with or without pcDNA3.1-CAV-1 transfection were treated with PB2 (25 μM) under HG conditions (25 mM) for 12 h. Cell proliferation was assessed by MTT assay. ROS generation was assessed using a ROS assay kit and H_2O_2 generation was assessed using a H_2O_2 detection kit, and the results were statistically analyzed. **P<0.01 vs. CT-HG; $^{\#\#}$P<0.01 vs. CT-HG + PB2 (25 μM). (D) Cells transfected with or without pcDNA3.1-CAV-1 were treated with PB2 (25 μM) under HG conditions (25 mM) for 12 h. The expression levels of redoxosome-related proteins were assessed by western blot analysis and statistically analyzed. **P<0.01 vs. CT-HG; $^{\#\#}$P<0.01 vs. CT-HG + PB2 (25 μM). All data are presented as the mean ± SD of three independent experiments. PB2, procyanidin B2; HG, high glucose; CAV-1, caveolin-1; p-, phosphorylated; NOX4, NADPH oxidase 4; CT, control; TF, CAV-1 transfection.

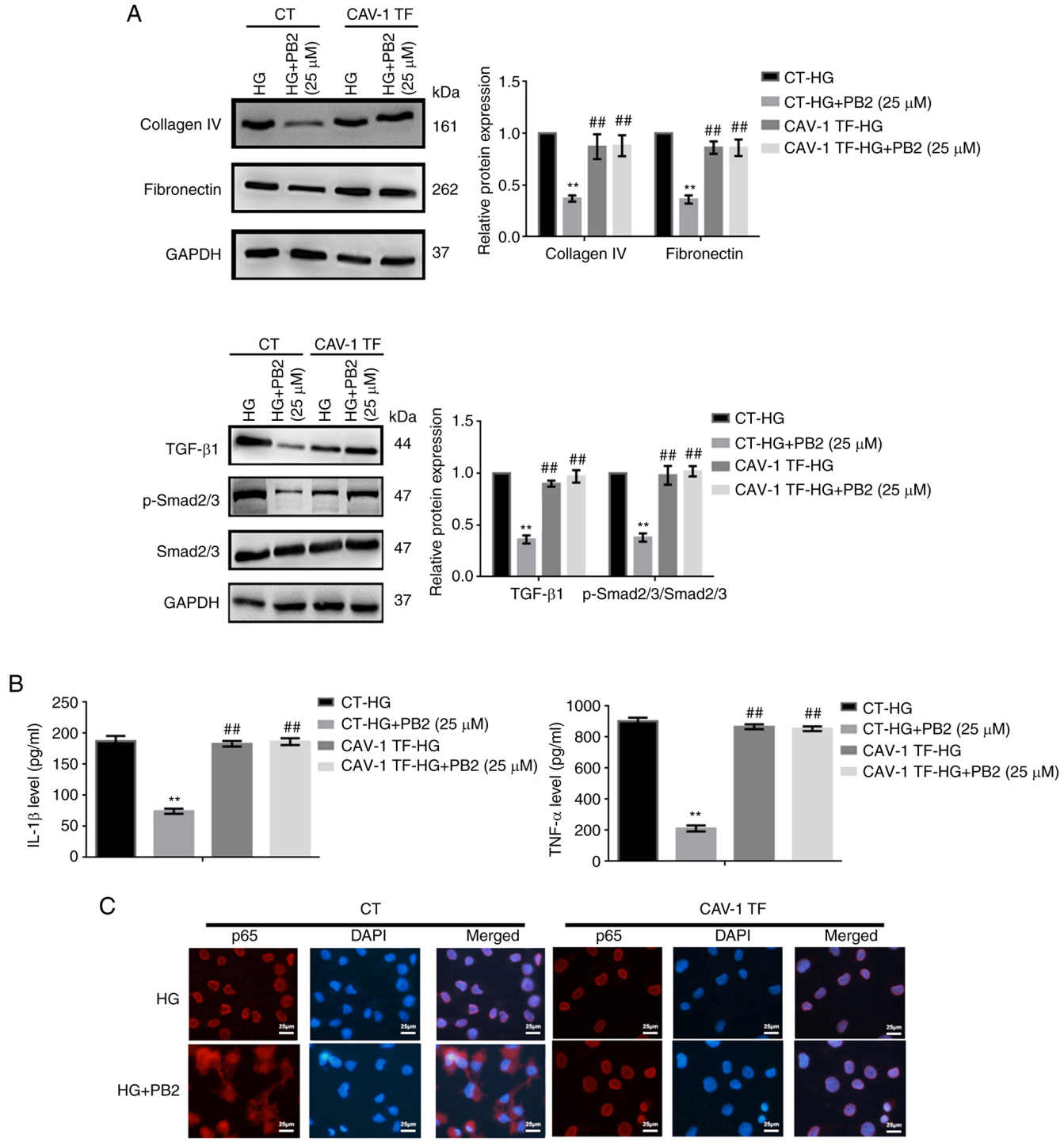

Figure 6. Effect of CAV-1 overexpression on the cytoprotective role of PB2 against extracellular matrix accumulation and inflammation in Mes13 cells. Cells transfected with or without CAV-1 were treated with PB2 (25 μM) under HG conditions (25 mM) for 12 h. (A) Expression levels of collagen IV and fibronectin, and TGF-β1/SMAD signaling-related proteins, were assessed by western blot analysis and statistically analyzed. (B) Levels of IL-1β and TNF-α were assessed by enzyme-linked immunosorbent assay and statistically analyzed. (C) Activation of NF-κB was assessed by immunofluorescence analysis. Scale bar, 25 μm. All data are presented as the mean ± SD of three independent experiments. **P<0.01 vs. CT-HG; $^{\#\#}$P<0.01 vs. CT-HG + PB2 (25 μM). PB2, procyanidin B2; HG, high glucose; CAV-1, caveolin-1; CT, control; TF, CAV-1 transfection.

Tukey's post hoc test among multiple groups. P<0.05 was considered to indicate a statistically significant difference.

Results

PB2 protects MCs against HG-induced cell proliferation and oxidative stress. To investigate the effect of PB2 on HG-induced MC dysfunction, Mes13 cells were treated with PB2 (5, 10, 25 and 50 μM) under HG conditions (25 mM). In the preliminary study, D-glucose (10, 25 and 30 mM) treatment at 37˚C for 12 h significantly induced rapid cell proliferation in Mes13 cells, as determined using MTT assay, whereas there was no significant difference between 25 and 30 mM concentrations (data not shown). Therefore,

the concentration of 25 mM D-glucose was chosen for subsequent experiments. In this study, cell proliferation was determined using the MTT assay, and oxidative stress was assessed using ROS and H_2O_2 analyses. As shown in Fig. 1, HG treatment significantly increased cell proliferation, and elevated ROS and H_2O_2 generation compared with the control group. However, PB2 treatment (10, 25 and 50 μM) treatment exerted protective effects on Mes13 cells under HG treatment, as determined by MTT assay, but there was no significant difference between the 25 and 50 μM concentrations. Therefore, the concentrations of 10 and 25 μM PB2 were chosen for assessing anti-oxidative effect. The results showed that PB2 treatment (10 and 25) dose-dependently attenuated elevated ROS and H_2O_2 generation induced by HG treatment.

PB2 protects MCs against oxidative stress by regulating redoxosomes signaling. To investigate the molecular mechanism underlying the cytoprotective effect of PB2 against oxidative stress in MCs, Mes13 cells were treated with PB2 (10 and 25 μM) under HG conditions (25 mM) and the expression levels of redoxosome-related proteins were assessed. As shown in Fig. 2A, HG treatment induced the upregulated expression of redoxosome-related proteins [RAC1/VAV2/NOX4] in cells, which may subsequently enhance ROS levels. However, PB2 treatment significantly attenuated such changes in Mes13 cells under HG conditions, which was similar to the effects of RAC1 inhibitor (NSC23766) and NOX inhibitor (VAS2870) (Fig. 2B). However, the effects of RAC1 inhibitor (NSC23766) or NOX inhibitor (VAS2870) on the expression of redoxosome-related proteins were not assessed.

PB2 protects MCs against HG-induced ECM accumulation by regulating TGF-β1/SMAD signaling. To investigate the effect of PB2 on HG-induced ECM accumulation in MCs, Mes13 cells were treated with PB2 (10 and 25 μM) under HG conditions (25 mM). ECM accumulation is a characteristic cellular response to HG (5). The expression of two typical ECM markers (collagen IV and fibronectin), as well as changes in TGF-β1/SMAD signaling were assessed. As shown in Fig. 3A and B, HG increased the expression levels of ECM proteins and activation of TGF-β1/SMAD signaling; however, PB2 treatment markedly attenuated ECM accumulation and inactivated TGF-β1/SMAD signaling in Mes13 cells under HG conditions. PB2 had similar effects to the TGF-β1/SMAD signaling inhibitor (LY2109761) with regard to ECM accumulation (Fig. 3C).

PB2 protects MCs against HG-induced inflammation by regulating NF-κB signaling. To investigate the effect of PB2 on HG-induced inflammation in MCs, Mes13 cells were treated with PB2 (10 and 25 μM) under HG conditions (25 mM). The levels of two typical cytokines (IL-1β and TNF-α) and the activation of NF-κB were assessed. As shown in Fig. 4, HG induced increased secretion of TNF-α and IL-1β, and activation of NF-κB signaling [translocation of p65 (NF-κB) from the cytoplasm to the nucleus]. However, PB2 treatment markedly reversed these phenotypes in Mes13 cells under HG conditions.

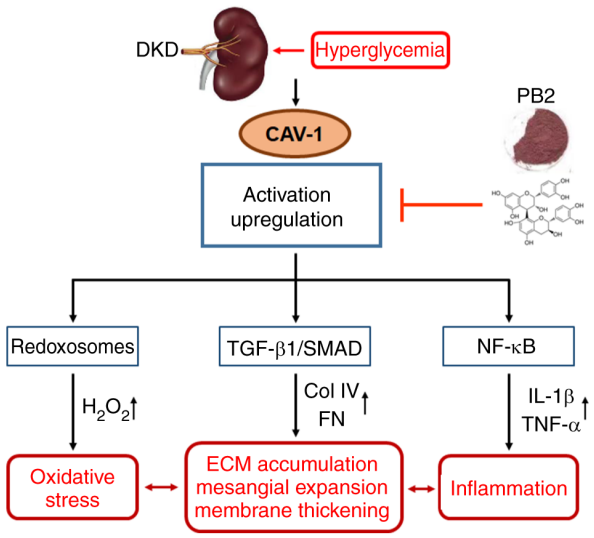

Figure 7. Diagram of the proposed mechanism underlying the protective effects of PB2 against hyperglycemia-induced mesangial cell dysfunction. PB2, procyanidin B2; DKD, diabetic kidney disease; ECM, extracellular matrix; CAV-1, caveolin-1; Col IV, type IV collagen; FN, fibronectin.

CAV-1 overexpression reverses the protective effect of PB2 on HG-induced MC dysfunction. CAV-1 is known to affect cellular redox homeostasis and inflammation in several cell lines. To investigate the key role of CAV-1 in the cytoprotective effect of PB2 on MCs, the expression and activation of CAV-1 were assessed. HG treatment enhanced CAV-1 expression levels and the phosphorylation of CAV-1 (Y14) in Mes13 cells (Fig. 5A). To further assess the role of CAV-1, Mes13 cells overexpressing CAV-1 were treated with PB2 (10 and 25 μM) under HG conditions (25 mM). CAV-1 overexpression could reverse the effects of PB2 on cell proliferation, oxidative stress, ECM accumulation and inflammation and the related signaling pathways (Figs. 5 and 6). The present data indicated that PB2 protected MCs against hyperglycemia by inactivating redoxosomes, and TGF-β1/SMAD and NF-κB signaling pathways in a CAV-1 dependent manner.

Discussion

PB2 has been reported to exert a variety of pharmacological effects on diabetic complications due to its antioxidative and anti-inflammatory activities (21,22). The renal protective effect of PB2 has been suggested in previous studies on animal models of diabetic nephropathy. Zhang *et al* (23) indicated PB2 as a prospective therapy, which could suppress MFG-E8, along with ERK1/2, Akt and GSK-3β signaling pathways. Li *et al* (24) reported that PB2 inhibited HG-induced epithelial-mesenchymal transition through the down-regulation of TGF-β/SMAD and mitogen-activated protein kinase/P38 signaling pathways in renal tubular epithelial cells. Bao *et al* (17) revealed that PB2 markedly ameliorated mitochondrial dysfunction and inhibited apoptosis in HG-treated rat MCs by activating the AMPK/SIRT1/PGC-1α axis. To the best of our knowledge, the present study was the first to reveal that PB2 exerted protective effects against hyperglycemia-induced MC dysfunction by attenuating cell proliferation, oxidative stress, ECM accumulation and inflammation.

Previous studies have revealed that CAV-1, in response to stimuli, can trigger MCs to secrete cytokines and produce ECM proteins (25,26). In DKD, CAV-1 has been reported to facilitate profibrotic signal transduction in response to several stimuli, including hyperglycemia and angiotensin II (27,28). The present study demonstrated that hyperglycemia upregulated and activated CAV-1 (CAV-1 phosphorylation) in MCs, which subsequently led to marked MC dysfunction. It is important to understand the role of CAV-1 in MC dysfunction under hyperglycemia. HG levels are known to stimulate redox signaling in renal MCs, which can lead to diabetic glomerular changes (29). Redoxosomes have recently been found to be a fledgling area of cellular signaling through superoxide-producing endosomes, which act via specific redox modifications on numerous proteins and enzymes (30,31). In the present study, using CAV-1 transfection experiments, it was revealed that redoxosomes were the downstream target of CAV-1, which control ROS generation and NF-κB activation. However, PB2 treatment significantly suppressed oxidative stress and inflammation induced by hyperglycemia, which may be via inhibiting CAV-1-dependent redoxosomes activation. These results indicated that CAV-1 was involved in redoxosomes signaling and may be a novel therapeutic target of DKD. The TGF-β1/SMAD signaling has an important role in renal fibrosis, the activation of which is crucial to the formation of the ECM (32,33). The present results indicated that CAV-1 could also activate TGF-β1/SMAD signaling, which may result in ECM accumulation in MCs under hyperglycemia. In addition, CAV-1 overexpression significantly reversed the effects of PB2 on TGF-β1/SMAD signaling and consequently ECM accumulation in MCs. Thus, CAV-1-dependent TGF-β1/SMAD signaling may also be a new therapeutic target of DKD (Fig. 7).

In conclusion, PB2 regulated the proliferation, oxidative stress, ECM accumulation and inflammation of glomerular MCs under hyperglycemia potentially by suppressing CAV-1-dependent signaling pathways. The present study suggested the potential clinical application of PB2 in treating DKD and indicated that CAV-1-related signaling pathways may be a potential therapeutic target of this disease.

Acknowledgements

Not applicable.

Funding

The present study was supported by the Project of Wuxi Health Commission (grant nos. Z202009, Z202014 and Z202110), the Key Project of Medical and Health Science and Technology Plan of Suzhou New District (grant no. 2019Z005) and the Science and Technology Development Project of Suzhou (grant no. SYSD2020087).

Availability of data and materials

The datasets used and/or analyzed during the current study are available from the corresponding author on reasonable request.

Authors' contributions

GL, DJ and FZ designed the experiments. JY, KW, XZ and JQ performed the experiments. JY, KW, XZ and JQ confirm the authenticity of all the raw data. JY and XZ analyzed the experimental results. JY and KW wrote the manuscript. All authors read and approved the final manuscript.

Ethics approval and consent to participate

Not applicable.

Patient consent for publication

Not applicable.

Competing interests

The authors declare that they have no competing interests.

References

1. Alicic RZ, Rooney MT and Tuttle KR: Diabetic kidney disease: Challenges, progress, and possibilities. Clin J Am Soc Nephrol 12: 2032-2045, 2017.
2. Lin YC, Chang YH, Yang SY, Wu KD and Chu TS: Update of pathophysiology and management of diabetic kidney disease. J Formos Med Assoc 117: 662-675, 2018.
3. Anders HJ, Huber TB, Isermann B and Schiffer M: CKD in diabetes: Diabetic kidney disease versus nondiabetic kidney disease. Nat Rev Nephrol 14: 361-377, 2018.
4. Zhao JH: Mesangial cells and renal fibrosis. Adv Exp Med Biol 1165: 165-194, 2019.
5. Dong Z, Sun Y, Wei G, Li S and Zhao Z: Ergosterol ameliorates diabetic nephropathy by attenuating mesangial cell proliferation and extracellular matrix deposition via the TGF-β1/Smad2 signaling pathway. Nutrients 11: 483, 2019.
6. Marciano DK: Mesangial cells: The tuft guys of glomerular development. J Am Soc Nephrol 30: 1551-1553, 2019.
7. Tung CW, Hsu YC, Shih YH, Chang PJ and Lin CL: Glomerular mesangial cell and podocyte injuries in diabetic nephropathy. Nephrology (Carlton) 23 (Suppl 4): S32-S37, 2018.
8. Parton RG, Tillu VA and Collins BM: Caveolae. Curr Biol 28: R402-R405, 2018.
9. Parton RG, McMahon KA and Wu Y: Caveolae: Formation, dynamics, and function. Curr Opin Cell Biol 65: 8-16, 2020.
10. Wang S, Wang N, Zheng Y, Zhang J, Zhang F and Wang Z: Caveolin-1: An oxidative stress-related target for cancer prevention. Oxid Med Cell Longev 2017: 7454031, 2017.
11. Peng F, Wu D, Ingram AJ, Zhang B, Gao B and Krepinsky JC: RhoA activation in mesangial cells by mechanical strain depends on caveolae and caveolin-1 interaction. J Am Soc Nephrol 18: 189-198, 2007.
12. Mehta N, Zhang D, Li R, Wang T, Gava A, Parthasarathy P, Gao B and Krepinsky JC: Caveolin-1 regulation of Sp1 controls production of the antifibrotic protein follistatin in kidney mesangial cells. Cell Commun Signal 17: 37, 2019.
13. Sun LN, Liu XC, Chen XJ, Guan GJ and Liu G: Curcumin attenuates high glucose-induced podocyte apoptosis by regulating functional connections between caveolin-1 phosphorylation and ROS. Acta Pharmacol Sin 37: 645-655, 2016.
14. Rauf A, Imran M, Abu-Izneid T, Iahtisham-Ul-Haq, Patel S, Pan X, Naz S, Sanches Silva A, Saeed F and Rasul Suleria HA: Proanthocyanidins: A comprehensive review. Biomed Pharmacother 116: 108999, 2019.
15. Luca SV, Macovei I, Bujor A, Miron A, Skalicka-Woźniak K, Aprotosoaie AC and Trifan A: Bioactivity of dietary polyphenols: The role of metabolites. Crit Rev Food Sci Nutr 60: 626-659, 2020.
16. Su H, Li Y, Hu D, Xie L, Ke H, Zheng X and Chen W: Procyanidin B2 ameliorates free fatty acids-induced hepatic steatosis through regulating TFEB-mediated lysosomal pathway and redox state. Free Radic Biol Med 126: 269-286, 2018.

17. Bao L, Cai X, Zhang Z and Li Y: Grape seed procyanidin B2 ameliorates mitochondrial dysfunction and inhibits apoptosis via the AMP-activated protein kinase-silent mating type information regulation 2 homologue 1-PPARγ co-activator-1α axis in rat mesangial cells under high-dose glucosamine. Br J Nutr 113: 35-44, 2014.
18. Zhou Y, Li BY, Li XL, Wang YJ, Zhang Z, Pei F, Wang QZ, Zhang J, Cai YW, Cheng M and Gao HQ: Restoration of mimecan expression by grape seed procyanidin B2 through regulation of nuclear factor-kappaB in mice with diabetic nephropathy. Iran J Kidney Dis 10: 325-331, 2016.
19. Breast Cancer Linkage Consortium: Cancer risks in BRCA2 mutation carriers. J Natl Cancer Inst 91: 1310-1316, 1999.
20. Chen B, Li Y, Liu Y and Xu Z: circLRP6 regulates high glucose-induced proliferation, oxidative stress, ECM accumulation, and inflammation in mesangial cells. J Cell Physiol 234: 21249-21259, 2019.
21. Fan J, Liu H, Wang J, Zeng J, Tan Y, Wang Y, Yu X, Li W, Wang P, Yang Z and Dai X: Procyanidin B2 improves endothelial progenitor cell function and promotes wound healing in diabetic mice via activating Nrf2. J Cell Mol Med 25: 652-665, 2021.
22. Yin M, Zhang P, Yu F, Zhang Z, Cai Q, Lu W, Li B, Qin W, Cheng M, Wang H and Gao H: Grape seed procyanidin B2 ameliorates hepatic lipid metabolism disorders in db/db mice. Mol Med Rep 16: 2844-2850, 2017.
23. Zhang Z, Li BY, Li XL, Cheng M, Yu F, Lu WD, Cai Q, Wang JF, Zhou RH, Gao HQ and Shen L: Proteomic analysis of kidney and protective effects of grape seed procyanidin B2 in db/db mice indicate MFG-E8 as a key molecule in the development of diabetic nephropathy. Biochim Biophys Acta 1832: 805-816, 2013.
24. Li D, Zhao T, Meng J, Jing Y, Jia F and He P: Procyanidin B2 inhibits high glucose-induced epithelial-mesenchymal transition in HK-2 human renal proximal tubular epithelial cells. Mol Med Rep 12: 8148-8154, 2015.
25. Adebiyi A, Soni H, John TA and Yang F: Lipid rafts are required for signal transduction by angiotensin II receptor type 1 in neonatal glomerular mesangial cells. Exp Cell Res 324: 92-104, 2014.
26. Guan TH, Chen G, Gao B, Janssen MR, Uttarwar L, Ingram AJ and Krepinsky JC: Caveolin-1 deficiency protects against mesangial matrix expansion in a mouse model of type 1 diabetic nephropathy. Diabetologia 56: 2068-2077, 2013.
27. Moriyama T, Tsuruta Y, Shimizu A, Itabashi M, Takei T, Horita S, Uchida K and Nitta K: The significance of caveolae in the glomeruli in glomerular disease. J Clin Pathol 64: 504-509, 2011.
28. Li CD, Zhao JY, Chen JL, Lu JH, Zhang MB, Huang Q, Cao YN, Jia GL, Tao YX, Li J and Cao H: Mechanism of the JAK2/STAT3-CAV-1-NR2B signaling pathway in painful diabetic neuropathy. Endocrine 64: 55-66, 2019.
29. Akaishi T, Abe M, Okuda H, Ishizawa K, Abe T, Ishii T and Ito S: High glucose level and angiotensin II type 1 receptor stimulation synergistically amplify oxidative stress in renal mesangial cells. Sci Rep 9: 5214, 2019.
30. Spencer NY and Engelhardt JF: The basic biology of redoxosomes in cytokine-mediated signal transduction and implications for disease-specific therapies. Biochemistry 53: 1551-1564, 2014.
31. Oakley FD, Abbott D, Li Q and Engelhardt JF: Signaling components of redox active endosomes: The redoxosomes. Antioxid Redox Signal 11: 1313-1333, 2009.
32. Dong J, Ding L, Wang L, Yang Z, Wang Y, Zang Y, Cao X and Tang L: Effects of bradykinin on proliferation, apoptosis, and cycle of glomerular mesangial cells via the TGF-β1/Smad signaling pathway. Turk J Biol 45: 17-25, 2021.
33. Ma TT and Meng XM: TGF-β/Smad and renal fibrosis. Adv Exp Med Biol 1165: 347-364, 2019.